ASEAN Engineering Journal

Full Paper

A COMPARISON OF POWER FLOW BASED ON BUS ADMITTANCE MATRIX FOR NETWORKED MICROGRID ENERGY MANAGEMENT

Halyani Mohd Yassim[a,b], Mohd Noor Abdullah[b]*, Chin Kim Gan[a]

[a]Faculty of Electrical Technology and Engineering, Universiti Teknikal Malaysia Melaka, 76100 Durian Tunggal, Melaka, Malaysia
[b]Green and Sustainable Energy (GSEnergy) Focus Group, Faculty of Electrical and Electronic Engineering, Universiti Tun Hussein Onn Malaysia, 86400 Batu Pahat, Johor, Malaysia

Article history
Received
18 June 2023
Received in revised form
15 September2023
Accepted
28 September2023
Published online
31 May 2024

*Corresponding author
mnoor@uthm.edu.my

Graphical abstract

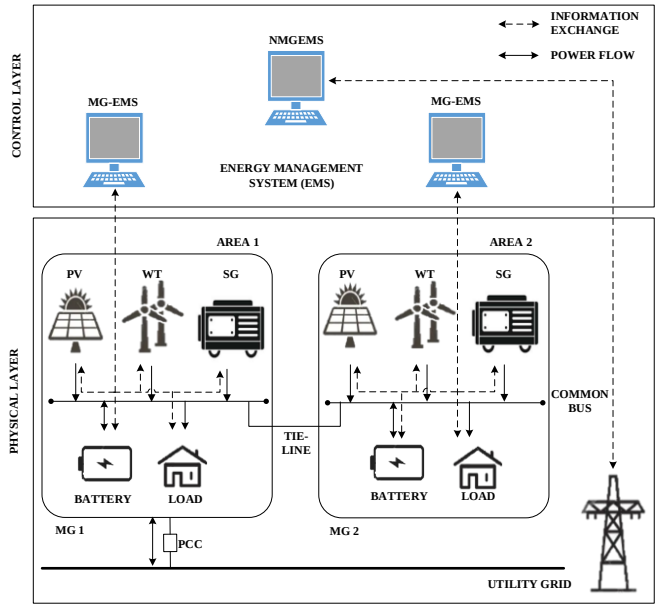

Abstract

A networked microgrid with an energy management system connects several microgrids to exchange power for cost-effective and reliable operation. The feasibility study is required as a basis for developing an efficient networked microgrid energy management plan. This paper presented a detailed power flow analysis of a networked microgrid. Multiple IEEE microgrids are interconnected in the networked microgrid system, and various types of distributed generators are modeled based on PQ and PV control schemes. Different power flow algorithms based on the bus admittance matrix are used in the MATLAB simulation. Several case studies demonstrated the feasibility of the networked microgrid in grid connected and islanded modes as well as the effectiveness of the Fast-Decoupled (BX version) method in facilitating power exchange between microgrids to maintain supply-demand balance under normal and abnormal conditions. The results proved that the Fast- Decoupled (BX version) method is significantly faster than the Fast- Decoupled (XB version) and Newton-Raphson methods and has better convergence than the Gauss-Seidel method.

Keywords: Distributed energy resources, energy management system, networked microgrid, power exchange, power flow analysis.

1.0 INTRODUCTION

To achieve sustainable development goals, access to affordable, reliable, and modern energy for all is a critical requirement, as about 840 million people mostly in South Asia, Sub-Saharan Africa, and Latin America live without electricity [1,2]. A microgrid (MG) is a promising way to organize distributed energy resources (DERs) to ensure a reliable power supply to meet the needs of rural communities [3–6]. However, an individual MG has a limited capacity to function as a reliable resource due to variations in renewable energy production. The concept of a networked microgrid (NMG) was introduced to enhance the MG's performance in grid connected and islanded modes. The flexibility of power exchange among several MGs can bring additional benefits to the system, such as increasing the use of renewable energy, system reliability, and cost-effectiveness [7–9]. The most important function in NMG is energy management [10], where power flow is required to ensure power balance in the system before making decisions about the best use of DERs to meet customer needs [11].

Power flow is one of the most important aspects of power system analysis. The knowledge of voltage magnitudes and angles of each bus of an electrical grid, as well as active and reactive power flows through its components (lines and transformers), provides an immediate picture of the steady-state power system. The power flow in NMGs is influenced by both operating modes (e.g., grid connected or islanded mode) and control modes (e.g., primary, secondary, and tertiary control) [12]. The utility grid controls the frequency of NMGs in grid-connected mode by means of the point of common coupling (PCC), while distributed generators (DGs) use the PQ and PV control schemes [13,14]. For NMGs islanded mode, decentralized droop control schemes are used to meet load demands while maintaining system frequency and bus voltages. In addition to droop controlled DGs, islanded NMGs also include DGs with PQ and PV control schemes [15,16]. Typical hierarchical NMG control includes the primary control, which deals with renewable DGs (RDGs) control using droop and non-droop control approaches; the secondary control, which deals with optimal operation of RDGs in each MG using central and decentralized methods; and the tertiary control, which deals with NMG energy management, including management of islanded MGs and the coordination of multiple MGs by considering the given objectives and constraints [17].

Power flow studies are based on two main approaches: bus impedance matrix and bus admittance matrix. The former approach is used in [18] to perform power flow analysis of balanced distribution systems with DGs, and in [19] to optimally control the amount of power exchange between two adjacent MGs. However, this approach requires a lot of computer memory, because the impedance bus is a full matrix of non-zero elements [20]. The latter approach is commonly used for many reasons. Since the admittance bus is a sparse matrix, it requires less computer memory. It is also simple to calculate and update in the event of any changes to the power system. Gauss-Seidel (GS) [21], Newton-Raphson (NR) [22], and Fast-Decoupled (FD) methods [23] are among power flow algorithms based on the bus admittance matrix. The FD method, which is a modification of the NR method, is fast and efficient.

Most of the researchers focused on NMG energy management system optimization. The results of static and dynamic power flow studies, which may be used as a reference for NMG energy management system optimization, were not thoroughly investigated. In addition, NMG energy management is also concerned with the computational burden (time and complexity). To solve AC power flow problems associated with energy management in various power system configurations, several power flow techniques have been proposed in the literature. The NR method is used in transmission systems with large-scale renewable generators [24], while the modified NR method is used in islanded AC MGs [11], and the backward-forward power flow method is used in NMG in active distribution networks [25] to obtain objective function parameters. However, the power flow method described in [25] is limited to a radial configuration network. The unidirectional power flow is the key characteristic of a radial distribution network. However, the expansion of RDGs requires meshed distribution networks for bidirectional power flow. The most relevant work is [26], which used the NR method to investigate the power flow analysis in NMG with radial and meshed distribution networks under normal conditions. However, the results of power flow analysis in abnormal conditions, such as a line outage and islanding MG, as well as the bidirectional power flow of energy storage systems (ESSs) are not discussed.

To the best of our knowledge, no literature has performed a power flow analysis of a 4-MG system using MATPOWER while accounting for ESS charging and discharging as well as abnormal MG operations. This paper compares the results of several case studies using GS, NR, and FD methods to determine the NMG system's feasibility prior to the implementation of an energy management plan. The contributions of the present work are summarized as follows:

1. Modeling a 4-MG system with RDGs and ESSs using MATPOWER.
2. Consideration of charging/discharging operation of the ESSs, the line outage, and islanding of the MG in the AC power flow problem.
3. Comparing the results of the GS, NR, and FD methods by using a 40-bus NMG system.

2.0 METHODOLOGY

The proposed NMG energy management plan includes power flow computation (see Figure 1). The MATPOWER function is used in the algorithm to analyze power flow and determine power losses in the network under consideration.

Figure 1 Block diagram of the proposed NMG energy management plan

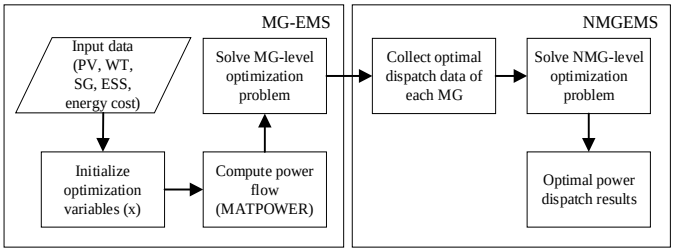

The procedure of NMG power flow analysis is broken down into five steps, which are described below. Firstly, this study was conducted by collecting data networks, which included line data, tie-line data, load data, generator data, and storage data. The data are obtained from the literature [26]. Resistance, reactance, and normal current rating of distribution lines are shown in Table 1. Table 2 shows tie-line data, while Table 3 shows load data for the NMG system. The bus type indicated in Table 3 for each bus contains the following information: a. Bus type 1: Slack bus; b. Bus type 2: PV bus; and c. Bus type 3: PQ bus. Table 4 provides information on RDGs installed at various MG locations, where the capacity of the inverter/converter installed is the same as shown in column 3 of Table 4. The data for synchronous generators and energy storage systems are shown in Tables 5 and 6.

Table 1 Line data of the NMG system [26]

No.	From bus	To bus	Resistance (Ω)	Reactance (Ω)	Normal rating (A)
1	B1	B2	0.09270	0.14310	1000
2	B1	B3	0.09336	0.11988	890
3	B1	B4	0.09270	0.14310	1000
4	B1	B5	0.06224	0.07992	890
5	B1	B6	0.06224	0.07992	890
6	B2	B3	0.07780	0.09990	890
7	B2	B5	0.05835	0.07493	890
8	B3	B4	0.07780	0.09990	890
9	B3	B5	0.04668	0.05994	890
10	B3	B6	0.04668	0.05994	890
11	B4	B6	0.05835	0.07493	890
12	B7	B8	0.05446	0.06993	890
13	B8	B9	0.06224	0.07992	890
14	B8	B12	0.23850	0.16200	310
15	B9	B10	0.08558	0.10989	890
16	B9	B13	0.22260	0.15120	310
17	B10	B11	0.07002	0.08991	890
18	B10	B14	0.04668	0.05994	890
19	B14	B15	0.12720	0.08640	310
20	B16	B17	0.04668	0.05994	890
21	B17	B18	0.07002	0.08991	890
22	B17	B24	0.05835	0.07493	890
23	B17	B26	0.22260	0.15120	310
24	B18	B19	0.04668	0.05994	890
25	B18	B28	0.23850	0.16200	310
26	B19	B20	0.05446	0.06993	890
27	B19	B29	0.22260	0.15120	310
28	B20	B21	0.06224	0.07992	890
29	B20	B30	0.22260	0.15120	310
30	B21	B22	0.05835	0.07493	890
31	B21	B32	0.22260	0.15120	310
32	B22	B23	0.23850	0.16200	310
33	B22	B33	0.06613	0.08492	890
34	B24	B25	0.05835	0.07493	890
35	B26	B27	0.19080	0.12960	310
36	B30	B31	0.19080	0.12960	310
37	B34	B35	0.03810	0.03150	700
38	B34	B38	0.06350	0.05250	700
39	B34	B39	0.11430	0.09450	700
40	B35	B36	0.12700	0.10500	700
41	B36	B37	0.03810	0.03150	700
42	B37	B40	0.06350	0.05250	700
43	B38	B39	0.09525	0.07875	700
44	B39	B40	0.09525	0.07875	700

Table 2 PCC/Tie-line data of the NMG system [26]

No.	From bus	To bus	Resistance (Ω)	Reactance (Ω)	Normal rating (A)
1	B2	B7	0.03090	0.04770	1000
2	B4	B16	0.04635	0.07155	1000
3	B14	B34	0.07780	0.09990	890
4	B11	B25	0.09725	0.12488	890
5	B33	B37	0.03890	0.04995	890

Table 3 Load data of the NMG system [26]

Bus no.	Bus type	Active power demand (kW)	Reactive power demand (kVAR)
B1	1	0	0
B2	2	2125	336
B3	2	3329	1023
B4	2	2050	555
B5	3	1257	310
B6	3	1056	240
B7	2	600	100
B8	2	1250	487
B9	2	1203	410
B10	2	1366	433
B11	3	764	36
B12	2	503	21
B13	3	345	11
B14	3	629	8
B15	2	642	12
B16	2	580	150
B17	3	650	85
B18	2	673	96
B19	2	439	135
B20	2	600	128
B21	2	560	112
B22	2	851	145
B23	3	420	25
B24	3	500	45
B25	3	637	33
B26	3	788	95
B27	3	125	50
B28	3	169	20
B29	2	200	43
B30	2	250	32
B31	3	213	12
B32	2	133	25
B33	3	200	38
B34	2	426	80
B35	3	318	78
B36	3	356	81
B37	3	459	88
B38	2	820	91
B39	2	2500	635
B40	2	816	60

Base voltage: 11 kV; Specified voltage at all buses: 1.0 p.u.

Table 4 Installed capacity of RDG in MGs of the system [26]

Bus no.	RDG type	Active power generation (kW)	Min. reactive power generation (kVAR)	Max. reactive power generation (kVAR)	Network area
B2	PV	2000	0	400	MG1
B3	PV	2400	0	480	MG1
B4	PV	2000	0	400	MG1
B8	PV	1600	0	320	MG2
B9	PV	1600	0	320	MG2
B10	PV	2400	0	480	MG2
B12	WT	800	-250	250	MG2
B15	WT	500	-200	200	MG2
B18	PV	2000	0	500	MG3
B19	PV	400	0	100	MG3
B20	PV	800	0	160	MG3
B21	PV	800	0	160	MG3
B22	PV	800	0	160	MG3
B29	WT	500	-250	250	MG3
B30	PV	800	0	160	MG3
B32	WT	1200	-600	600	MG3
B38	PV	1600	0	320	MG4
B39	PV	2400	0	500	MG4
B40	PV	1600	0	320	MG4

Table 5 Standby synchronous generator data in MGs of the system [26]

Bus no.	Unit capacity (kVA)	Number of units	Min. reactive power generation (kVAR)	Max. reactive power generation (kVAR)	Network area
B1	5000	3	-3000	5000	MG1
B7	2000	3	-1500	2000	MG2
B16	2000	3	-1500	2000	MG3
B34	2000	2	-1000	2000	MG4

Table 6 Energy storage capacity [26]

Bus no.	Battery storage capacity (kWh)	Peak power supply (kW)	Network area
B2	3000	2000	MG1
B3	4000	2400	MG1
B4	3000	2000	MG1
B8	4000	1600	MG2
B9	4000	1600	MG2
B10	4000	2400	MG2
B18	3600	2000	MG3
B19	800	400	MG3
B20	2000	800	MG3
B21	2000	800	MG3
B22	2000	800	MG3
B30	2000	800	MG3
B38	3000	1600	MG4
B39	6000	2400	MG4
B40	3000	1600	MG4

Next, an NMG system, as shown in Figure 2, with synchronous generators (SGs), photovoltaic solar panels (PVs), wind turbines (WTs), and ESSs was modeled into several IEEE bus systems in MATLAB using MATPOWER. The MATPOWER case file was modified based on the data collection for NMG modeling. A modified IEEE 6-bus, 33-bus, 69-bus, and 14-bus system was then connected via point of common couplings (PCC1, PCC2, PCC3, PCC4, PCC5) to form a fully meshed NMG with four MGs. When in grid-connected mode, MG1 is directly connected to the utility grid. The utility grid is modeled as a slack bus in grid-connected mode to maintain load balance and voltage control for the entire system. When breaker Br opens, MG1 is switched to islanded mode. A conventional SG acts as a slack bus in islanded mode to provide load balancing and reactive power support. The PV and WT installed in the MGs are specified by a constant power factor model (power factor = 1.0). The buses connected to the constant power factor generators are referred to as PQ buses. The buses connected to constant voltage generators e.g. ESSs are referred to as PV buses.

The network topology was then visualized using a web-based visualization tool called Steady-State AC Network Visualization. To test the system's feasibility, a power flow analysis was then carried out in several case studies of grid connected and islanded NMG using GS, NR, and FD methods. The complex power flow equations for AC NMG model can be expressed as a nonlinear function [27]:

$$P_j = V_j \sum_{n=1}^{N} V_n \left[G_{jn} \cos\left(\delta_j - \delta_n\right) + B_{jn} \sin\left(\delta_j - \delta_n\right) \right] \quad (1)$$

$$Q_j = V_j \sum_{n=1}^{N} V_n \left[G_{jn} \sin\left(\delta_j - \delta_n\right) - B_{jn} \cos\left(\delta_j - \delta_n\right) \right] \quad (2)$$

Equations (1) and (2) describe the active and reactive power supplied to bus j (P_j and Q_j) respectively, and are based on nodal equations, in which N is the maximum number of buses, V_j and δj are the voltage magnitude and phase angle at bus j, and G_{jn} and B_{jn} are the real and imaginary parts of the bus admittance matrix element associated with buses j and n. If a power flow analysis is not feasible, the network parameters are modified accordingly. The power flow results were discussed in detail, and the most efficient power flow technique was chosen for this study. Figure 3 illustrates the procedures of NMG power flow analysis.

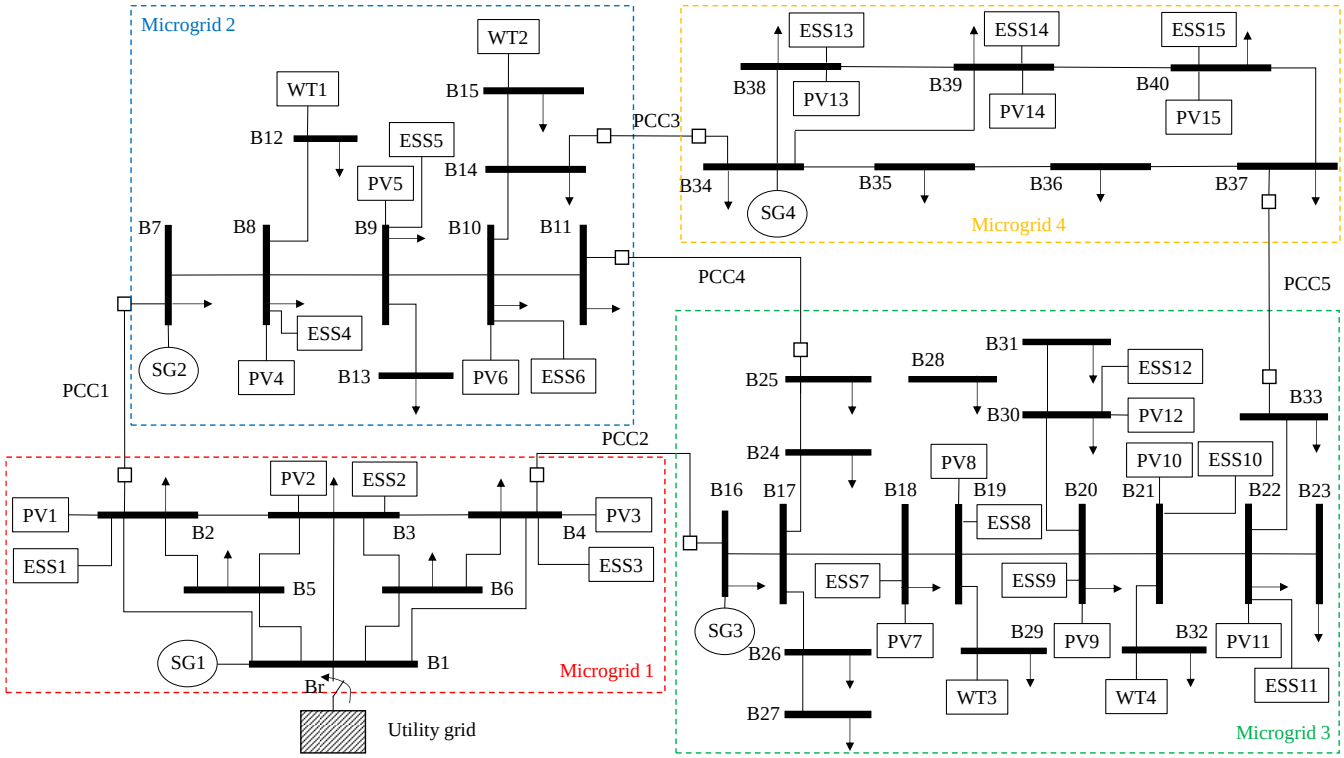

Figure 2 Single-line diagram of the NMG system

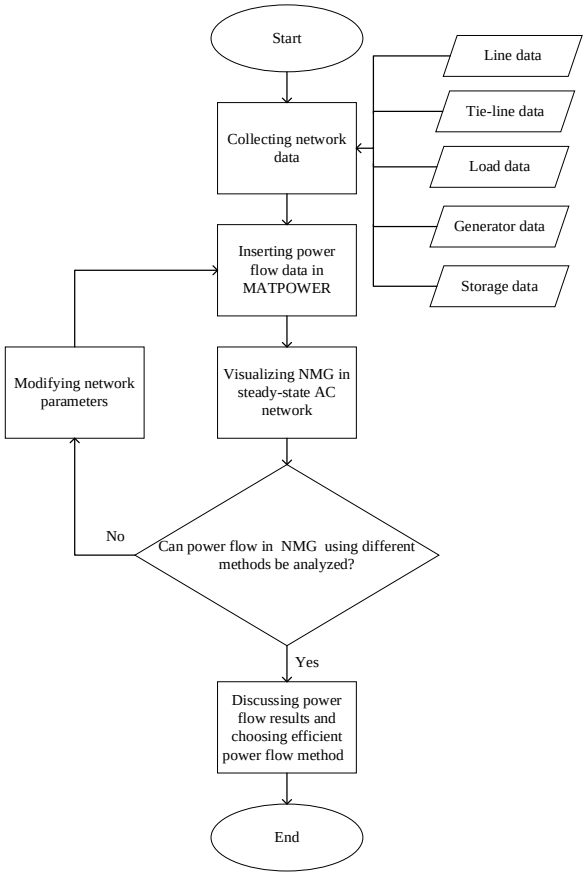

Figure 3 Flowchart of NMG power flow analysis

3.0 RESULTS AND DISCUSSION

The FD algorithms (XB and BX versions) are tested on a 40-bus NMG system, and power flow results are obtained. A comparison of computation performance between other power flow algorithms is also presented here.

The test system, as shown in Figure 2, has one feeder and 40 buses. Only MG1 is connected to the utility feeder. MG2 and MG3 can receive power from MG1, while MG4 can receive power from MG2 and/or MG3. In Table 7, five different scenarios are shown. These scenarios are based on supply and load demand on 7th day (Sunday) and 12th week of the year, as shown in Figure 4 [26]. Scenarios 1, 2, and 5 simulate NMG operations in grid-connected mode. In such cases, the utility grid meets the major portion of the total system load demand, with the remaining portion being met by local WTs, PVs, or ESS units. Scenarios 3 and 4 simulate NMG operations in islanded mode. Most of the loads are shared by local PVs and WTs. The surplus power is stored in an ESS connected to a PV system and used to power each MG during the peak load demand. SGs are also used to provide reactive power support to the MG in islanded mode.

Table 7 Test scenarios

Scenario	Time (hour)	Total load (kW)	Total power supply (kW)			PCC/Br open	Remarks
			PV	WT	ESS		
1	01:00	15023	0	1140	0	-	Min. load
2	08:00	17755	9512	1860	0	-	Line outage
3	10:00	20259	17632	2010	0	1,3,4, Br	Islanding MG2
4	14:00	19576	23200	1530	0	4,5, Br	Max. PV
5	19:00	22763	0	2130	4123	-	Peak load

3.1 Computational Performance

The power flow analysis was performed in MATLAB version R2021a on a 64-bit computer with an AMD Ryzen 7 CPU 4700U 2.00 GHz, and 8 GB RAM, using GS, NR, FDBX, and FDXB methods. Table 8 highlights the computational performance of each scenario. The maximum allowed power mismatch is set to 10-8 per unit, with a maximum iteration number of 2000. The FDBX method obtained the final solution with the required precision in 22.5 ms and 8 iterations by using scenario 1 as an example. To find the solution with the same precision, the FDXB method took 109.6 ms and 6 iterations, the NR method took 268.9 ms and 3 iterations, and the GS method took 268.2 ms and 1093 iterations. For other scenarios, similar results can be found in the same table, except that in scenarios 2 and 3, the GS method failed to converge to a solution with the maximum number of iterations allowed. In scenario2, the algorithm had to recalculate the new elements of the bus admittance matrix, specifically Y_1010, Y_1414, and Y_1014, while in scenario 3, the algorithm had to calculate multiple power flows of two islanded systems, namely island 1 (MG1, MG3, MG4) and island 2 (MG2). On the other hand, the circuit reconfiguration, and the presence of ESS in scenarios 3-5 increased the number of iterations required for FDXB methods to converge within specific limits. The FDBX method, according to the Table 8, is more efficient than the FDXB, NR, and GS methods. As a result, the FDBX method is considered as a power flow solution approach for this NMG system.

Table 8 Comparison of convergence characteristics

Scenario	No. of iterations				CPU time (ms)			
	GS	NR	FDXB	FDBX	GS	NR	FDXB	FDBX
1	1093	3	6	8	268.2	268.9	109.6	22.5
2	2000*	3	7	8	433.9	56.7	13.9	8.2
3	2000*	2	18	6	461.1	77.2	29.0	8.3
4	1406	3	16	6	315.5	40.3	10.7	4.4
5	1199	3	23	7	297.6	20.5	8.0	5.6

*: GS method does not converge

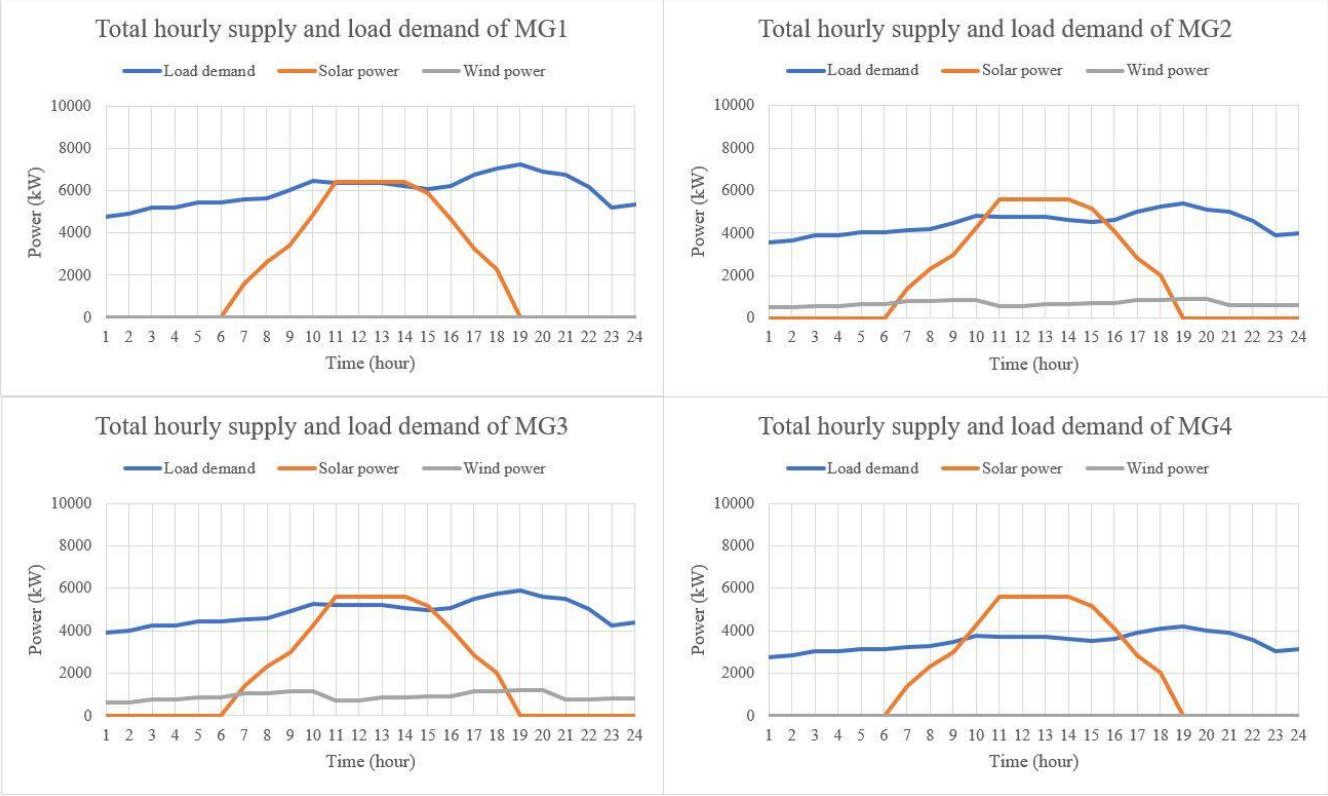

Figure 4 Total hourly supply and load demand of MGs in the system

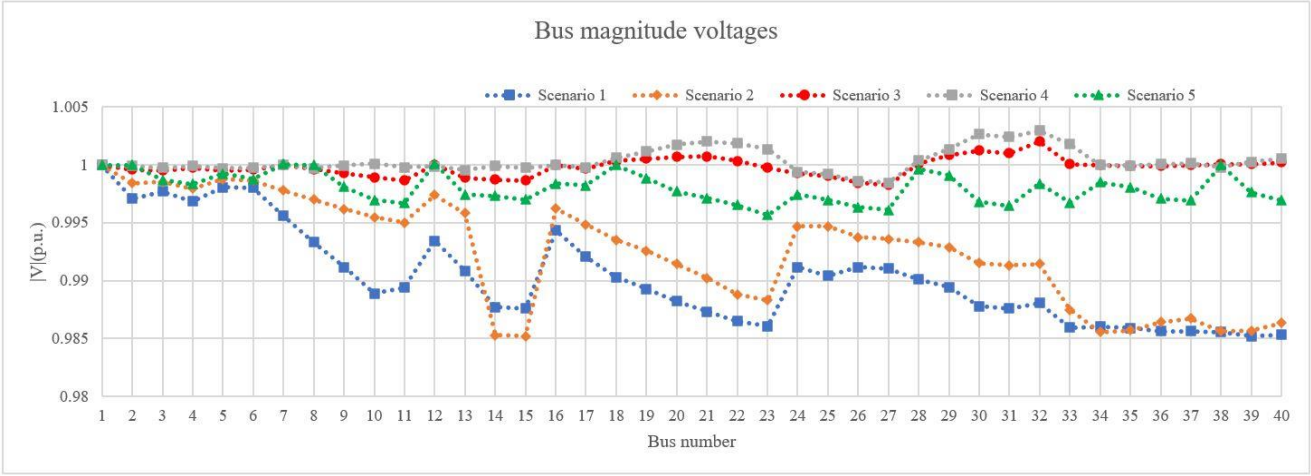

Figure 5 Voltage profile of the five considered scenarios

3.2 Voltage Profile

The bus magnitude voltages for all scenarios are shown in Figure 5. In scenarios 1 and 2, there is a significant voltage drop due to the power supply and demand imbalances in the grid system, which are exacerbated by utility power plants located far from the load centers [28]. A line outage in B10-B14 also results in a voltage drop in B14-B15. In scenarios 3 and 4, the presence of small RDGs near local loads greatly raises the voltage profile. In contrast to scenarios 1 and 2, the presence of ESS in scenario 5 also helps to improve the voltage profile by providing reactive power support to the system.

3.3 Power Flow Exchange And Power Losses

Tables 9-13 shows the active power flow exchanges for all scenarios. In scenario 1, MG1 imports 13977 kW from the utility grid because the system's load demand exceeds WT generation. MG2 receives 4214 kW of power from MG1, while MG3 receives 4943 kW of power from MG1. MG4 receives 2071 kW from MG2 and 710 kW from MG3. MG3 shares 951 kW with MG2 to maintain the system's power balance. 94 kW of total power losses are recorded. In scenario 2, the amount of power imported from the utility grid and total power losses are reduced due to the presence of PV units, which contribute a small amount to meet load demands. Scenario 3 consists of two islanded systems: island 1 (MG1, MG3, MG4), and island 2 (MG2). SGs perform load balancing and reactive power support at each MG. The majority of load demands are met by WT and PV units. The ESS is programmed to charge based on the excess WT and PV power generated by each MG. The initial state of the ESS is assumed to be based on one-day cycles and is set to 0 kWh. In each MG2, MG3, and MG4, only one ESS is required to charge 324 kW, 141 kW, and 510 kW power. MG3 receives 8 kW from MG1 and shares about 0.4 kW with MG4 to maintain the system's power balance.

The maximum power of ESS 161 kW, 1622 kW, 1390 kW, and 1981 kW are stored in MG1, MG, MG3, and MG4, respectively, at 14:00 hours (scenario 4) during peak PV generation. However, only 80% (i.e. depth of discharge requirement) of the power stored in scenario 4 is discharged during scenario 5 to extend the life span of the ESS. The ESS is used during this period to reduce the peak load demand, which can reduce the load factor and consequently reduce the electricity bill. MG1 imports 24937 kW from the utility grid because the maximum load demand in the system exceeds WT power generation and ESS power discharge. MG2 receives 6725 kW of power from MG1, while MG3 receives 8397 kW of power from MG1. MG4 receives 3137 kW from MG2 and 1008 kW from MG3. MG3 receives 1591 kW from MG2 to maintain the system's power balance. 388 kW of total power losses are recorded.

Table 9 Power flow exchanges in scenario 1

Time 01:00		**MG1 (kW)**	**MG2 (kW)**	**MG3 (kW)**	**MG4 (kW)**	**NMG (kW)**
SG		Standby mode				
ESS		Idle mode				
PV		0	0	0	0	0
WT			494	646		1140
Load		4788	3561	3896	2778	15023
MGs' status		Shortage				
Power exchange	Grid	-13977				NMG is balanced after power exchange
	MG1		-4214	-4943		
	MG2	4214		951	-2071	
	MG3	4943	-951		-710	
	MG4		2071	710		

Table 10 Power flow exchanges in scenario 2

Time 08:00		**MG1 (kW)**	**MG2 (kW)**	**MG3 (kW)**	**MG4 (kW)**	**NMG (kW)**
SG		Standby mode				
ESS		Idle mode				
PV		2624	2296	2296	2296	9512
WT			806	1054		1860
Load		5659	4209	4604	3283	17755
MGs' status		Shortage				
Power exchange	Grid	-6410				NMG is balanced after power exchange
	MG1		-1047	-2320		
	MG2	1047		361	423	
	MG3	2320	-361		-1411	
	MG4		-423	1411		

Table 11 Power flow exchanges in scenario 3

Time 10:00		MG1 (kW)	MG2 (kW)	MG3 (kW)	MG4 (kW)	NMG (kW)
SG		1602	1	0	0	1603
ESS		0	-324	-141	-510	-975
PV		4864	4256	4256	4256	17632
WT			871	1139		2010
Load		6457	4803	5254	3745	20259
MGs' status		Shortage	Surplus			
Power exchange	Grid					NMG is balanced after power exchange
	MG1			-8		
	MG2					
	MG3	8			-0[a]	
	MG4			0[a]		

[a]: Power exchange is too small (0.4 kW)

Table 12 Power flow exchanges in scenario 4

Time 14:00		MG1 (kW)	MG2 (kW)	MG3 (kW)	MG4 (kW)	NMG (kW)
SG		12	0	0	0	12
ESS		-161	-1622	-1390	-1981	-5154
PV		6400	5600	5600	5600	23200
WT			663	867		1530
Load		6239	4641	5077	3619	19576
MGs' status		Surplus				
Power exchange	Grid					NMG is balanced after power exchange
	MG1		-3	-9		
	MG2	3			-1	
	MG3	9				
	MG4		1			

Table 13 Power flow exchanges in scenario 5

Time 19:00		MG1 (kW)	MG2 (kW)	MG3 (kW)	MG4 (kW)	NMG (kW)
SG		Standby mode				
ESS		129	1297	1112	1585	4123
PV		0	0	0	0	0
WT			923	1207		2130
Load		7255	5396	5903	4209	22763
MGs' status		Shortage				
Power exchange	Grid	-24937				NMG is balanced after power exchange
	MG1		-6725	-8397		
	MG2	6725		-1591	-3137	
	MG3	8397	1591		-1008	
	MG4		3137	1008		

4.0 CONCLUSION

This study included a detailed analysis of the power flow study of an NMG that consists of four MGs that can operate with or without connection to the LV distribution system. Several operational scenarios are investigated, including economic dispatch, load changes, line outages, operational mode transition, and bidirectional power flow. The case studies demonstrated the operational feasibility of NMGs in electrical distribution systems, as well as the effectiveness of the FDBX method in facilitating power exchange between MGs to maintain supply-demand balance under normal and abnormal conditions. Future work will focus on optimizing power flow exchanges and ESS to achieve both economic objectives and operational safety requirements.

Acknowledgement

This research was supported by Universiti Tun Hussein Onn Malaysia through TIER 1 Research Grant (Q360) and Universiti Teknikal Malaysia Melaka.

References

[1] United Nations, Take action for the sustainable development goals. Retrieved from https://www.un.org/sustainabledevelopment/sustainable-development-goals/ Retrieved on 23 May 2023

[2] IEA, Energy access: Achieving modern energy for all by 2030 seems unlikely. Retrieved from https://www.iea.org/topics/energy-access

[3] Li, J., Y. Liu, and L. Wu. 2018. Optimal operation for community-based multi-party microgrid in grid-connected and Islanded modes. *IEEE Trans Smart Grid*. 9(2): 756–765. DOI: 10.1109/TSG.2016.2564645

[4] Hirsch, A., Y. Parag, and J. Guerrero. 2018. Microgrids: A review of technologies, key drivers, and outstanding issues. *Renewable and Sustainable Energy Reviews*. 90: 402–411. DOI: 10.1016/j.rser.2018.03.040

[5] Sandelic, M., S. Peyghami, A. Sangwongwanich, and F. Blaabjerg. 2022. Reliability aspects in microgrid design and planning: Status and power electronics-induced challenges. *Renewable and Sustainable Energy Reviews*. 159: 112127. DOI: 10.1016/j.rser.2022.112127

[6] Cabello, G. M., S. J. Navas, I. M. Vázquez, A. Iranzo, and F. J. Pino. 2022. Renewable medium-small projects in Spain: Past and present of microgrid development. *Renewable and Sustainable Energy Reviews.* 165: 112622. DOI: 10.1016/j.rser.2022.112622

[7] Vosoogh, M., M. Rashidinejad, A. Abdollahi, and M. Ghaseminezhad. 2021. An intelligent day ahead energy management framework for networked microgrids considering high penetration of electric vehicles. *IEEE Trans Industr Inform.* 17(1): 667–677. DOI: 10.1109/TII.2020.2977989

[8] Cao, Y. et al. 2022. Optimal energy management for multi-microgrid under a transactive energy framework with distributionally robust optimization. *IEEE Trans Smart Grid*. 13(1): 599–612. DOI: 10.1109/TSG.2021.3113573

[9] Jia, Y., P. Wen, Y. Yan, and L. Huo. 2021. Joint operation and transaction mode of rural multi microgrid and distribution network. *IEEE Access*. 9: 14409–14421. DOI: 10.1109/ACCESS.2021.3050793

[10] Ahmad, S., M. Shafiullah, C. B. Ahmed, and M. Alowaifeer. 2023. A review of microgrid energy management and control strategies. *IEEE Access*. 1–34. DOI: 10.1109/ACCESS.2023.3248511

[11] Chopra, S., G. M. Vanaprasad, G. D. A. Tinajero, N. Bazmohammadi, J. C. Vasquez, and J. M. Guerrero. 2022. Power-flow-based energy management of hierarchically controlled islanded AC microgrids. *International Journal of Electrical Power and Energy Systems*. 141(September 2021): 108140. DOI: 10.1016/j.ijepes.2022.108140

[12] Feng, F., P. Zhang, Y. Zhou, and L. Wang. 2023. Distributed Networked Microgrids Power Flow. *IEEE Transactions on Power Systems*. 38(2): 1405–1419. DOI: 10.1109/TPWRS.2022.3175933

[13] Kumar, A., B. K. Jha, S. Das, and R. Mallipeddi. 2021. Power flow analysis of islanded microgrids: A differential evolution approach. *IEEE Access*. 9: 61721–61738. DOI: 10.1109/ACCESS.2021.3073509

[14] Eto, J. H. et al. 2018. The CERTS microgrid concept, as demonstrated at the CERTS/AEP Microgrid Test Bed.

[15] Xu, Z., P. Yang, C. Zheng, Y. Zhang, J. Peng, and Z. Zeng. 2018. Analysis on the organization and development of multi-microgrids. *Renewable*

and Sustainable Energy Reviews. 81: 2204–2216. DOI: 10.1016/j.rser.2017.06.032

[16] Sadek, S. M., W. A. Omran, M. A. M. Hassan, and H. E. A. Talaat. 2021. Adaptive robust energy management for isolated microgrids considering reactive power capabilities of distributed energy resources and reactive power costs. *Electric Power Systems Research*. 199: 5397–5411.DOI: 10.1016/j.epsr.2021.107375

[17] Moradi, M. H., V. B. Foroutan, and M. Abedini. 2017. Power flow analysis in islanded Micro-Grids via modeling different operational modes of DGs: A review and a new approach. *Renewable and Sustainable Energy Reviews*. 69(August 2015): 248–262. DOI: 10.1016/j.rser.2016.11.156

[18] Sun, H., D. Nikovski, T. Ohno, T. Takano, and Y. Kojima. 2011. A fast and robust load flow method for distribution systems with distributed generations. *Energy Procedia.* 12: 236–244. DOI: 10.1016/j.egypro.2011.10.033

[19] Kargarian, A., and M. Rahmani. 2015. Multi-microgrid energy systems operation incorporating distribution-interline power flow controller. *Electric Power Systems Research*. 129: 208–216. DOI: 10.1016/j.epsr.2015.08.015

[20] Benato, R. 2022. A basic AC power flow based on the bus admittance matrix incorporating loads and generators including slack bus. *IEEE Transactions on Power Systems*. 37(2): 1363–1374. DOI: 10.1109/TPWRS.2021.3104097

[21] Glimn, A. F., and G. W. Stagg. 1957. Automatic calculation of load flows. *Transactions of the American Institute of Electrical Engineers*. *Part III: Power Apparatus and Systems.* 76(3): 817–825. Retrieved from https://ieeexplore.ieee.org.libproxy.utem.edu.my/stamp/stamp.jsp?tp=&arnumber=4499665

[22] Tinney, W. F., and C. E. Hart. 1967. Power flow solution by Newton's method. *IEEE Transactions on Power Apparatus and Systems.* PAS-86(11): 1449–1460. Retrieved from https://ieeexplore.ieee.org.libproxy.utem.edu.my/stamp/stamp.jsp?tp=&arnumber=4073219 Retrieved on 16 March 2023

[23] Stott, B., and O. Alsac. 1974. Fast decoupled load flow. *IEEE Transactions on Power Apparatus and Systems*. PAS-93(3): 859–869. DOI : 10.1109/TPAS.1974.293985

[24] Biswas, P. P., P. N. Suganthan, B. Y. Qu, and G. A. J. Amaratunga. 2018. Multiobjective economic-environmental power dispatch with stochastic wind-solar-small hydro power. *Energy*. 150: 1039–1057. DOI: 10.1016/j.energy.2018.03.002

[25] Haddadian, H., and R. Noroozian. 2019. Multi-microgrid-based operation of active distribution networks considering demand response programs. *IEEE Trans Sustain Energy*. 10(4): 1804–1812. DOI: 10.1109/TSTE.2018.2873206

[26] Alam, M. N., S. Chakrabarti, and X. Liang. 2020. A benchmark test system for networked microgrids. *IEEE Trans Industr Inform*. 16(10): 6217–6230. DOI: 10.1109/TII.2020.2976893

[27] Glover, J. D., M. S. Sarma, and T. J. Overbye. 2010. *Power system analysis and design*. USA: Global Engineering.

[28] Kang, H., S. Jung, M. Lee, and T. Hong. 2022. How to better share energy towards a carbon-neutral city? A review on application strategies of battery energy storage system in city. *Renewable and Sustainable Energy Reviews*. 157: 1–21. DOI: 10.1016/B978-0-323-60984-5.00062-7